BIOLOGY Methods & Protocols

Biology Methods and Protocols, 2021, 1–7

doi: 10.1093/biomethods/bpab002
Advance Access Publication Date: 9 February 2021
Innovations

INNOVATIONS

Single well, single-common primer pair, dual probe, duplex qPCR assay for the quantification of mRNA splicing variants

Janice Wang,[1,†] Winifred P. Wong,[1,†] Emma O. Link,[2] Shantel Olivares,[3] Cade T. Adelman,[1,4] Anne S. Henkel[3] and Malek El Muayed[1,*]

[1]Division of Endocrinology, Metabolism and Molecular Medicine, Feinberg School of Medicine, Northwestern University, Chicago, IL 60611, USA, [2] Masters of Biomedical Studies Program, Drexel University, Philadelphia, PA 19104, USA, [3]Division of Gastroenterology and Hepatology, Department of Medicine, Feinberg School of Medicine, Northwestern University, Chicago, IL 60611, USA and [4]Department of Biomedical Engineering, George Washington University School of Engineering and Applied Sciences, Washington, DC 20052, USA

[†]These authors contributed equally to this work.
*Correspondence address. Division of Endocrinology, Metabolism and Molecular Medicine, Feinberg School of Medicine, Northwestern University, Chicago, IL, USA. E-mail: m-muayed@northwestern.edu

Abstract

Quantifying the ratio of alternatively spliced mRNA variants of genes with known alternative splicing variants is highly relevant for many applications. Herein, we describe the validation of a quantitative PCR design for the simplified quantification of known mRNA splice variants. The assay uses a single-common primer pair, dual probe design for the determination of splicing variants in a single well configuration. We used murine XBP-1 splicing variants, XBP-1S and XBP-1U, to validate and demonstrate the performance characteristics of this approach. Using synthetic XBP-1S and XBP-1U cDNA as well as cDNA synthesized from mouse beta-cell line MIN6, we established the performance parameters and dynamic range of the assay. Reliable quantification of both variants at varying concentration gradients was shown. No cross detection of XBP-1U by the XBP-1S probe was detected and only marginal XBP-1S cross detection by the XBP-1U probe was detected at high concentration gradients that are unlikely to be relevant. We demonstrated that the assay accurately detected changes of XBP-1 splice variants in mouse liver subjected to pharmacologically induced ER stress without the need for normalization to a reference gene.

Keywords: XBP-1; single primer pair; common primer pair; qPCR; duplex qPCR; PCR probe; splice variant quantification

Introduction

The accurate quantification of splicing variants of alternatively spliced genes is of high importance for various research applications. It is relevant for several research areas including neoplastic disorders [1], neurologic disorders [2], renal disease and angiogenesis [3], senescence and aging [4], as well as endoplasmic reticulum (ER) stress X-box binding protein 1 (XBP-1) [5]. Traditionally, quantifying relative splice variant concentrations

Received: 17 December 2020; **Revised:** 31 January 2021; **Editorial Decision:** 1 February 2021; **Accepted:** 5 February 2021

has been accomplished using semi-quantitative PCR (qPCR) followed by gel electrophoresis and Western blotting of protein products (in the case of translated splice variants). qPCR has increasingly been used for this purpose [6–9]. Traditionally, qPCR assays are designed using different primer pairs specific to each splicing variant, followed by detection with either an intercalating dye or a probe. Several groups sought to improve on these methods by seeking to establish duplex or multiplex, sample assays capable of quantifying several splice variants in one sample without the need for separate samples for the detection of each splice variants. To that end, Camacho *et al.* [10] described a method using splice site-specific amplification and melt curve analysis. Sun *et al.* [11] and Sun and Zheng [12] previously reported a droplet digital PCR (ddPCR) to identify splice variants of human telomerase reverse transcriptase (hTERT) using a single primer pair and specific hydrolysis probes with distinct dyes. Herein, we provide proof of concept of a common primer pair, dual probe assay for the detection of two splicing variants of the XBP-1 gene using qPCR. In this qPCR setup, the common primer pair flanking the alternative splice site is used for the amplification of both splicing variants. Detection specificity is achieved using two distinct hydrolysis probes specific to each splicing variant, enabling single well amplification and detection of both variants (Fig. 1). The method, we describe here is similar in its conceptual design to the method of Sun *et al.* [11] and Sun and Zheng [12]. Significant inherent differences exist between ddPCR and qPCR. While the dPCR method is more sensitive and precise, it is also more complex and expensive. qPCR provides far greater dynamic detection range but it also exhibits higher susceptibility to interfering substances. The technical characteristics of qPCR make it imperative to validate the assay to establish the relative amplification efficacy for each splice variant while also ensuring no significant cross reactivity.

The proportion of classically spliced (U) and alternatively spliced (S) XBP-1 mRNA is accepted as a good reporter for estimating ER stress in the acute phase [5]. However, accurately quantifying the ratio between the S and U splice variants of XBP-1 (XBP-1S and XBP-1U) is challenging. This approach is intended to simplify the quantification of both splicing variants using qPCR. It is likely that this approach can also be adapted to settings where more than two splice variants are investigated.

Materials and methods

Assay description

Herein, we report the validation and performance characteristics of a newly designed single primer pair, dual probe-based qPCR assay for determining the ratio of both splicing variants of mouse XBP-1 in a single well, duplex configuration. The assay uses a common primer pair for amplification (Table 1), while using two distinct fluorescent hydrolysis probes hexachlorofluorescein (HEX) and fluorescein amidite (FAM) with appropriate quenchers specific for each of the amplicons generated by XBP-1S and XBP-1U splicing variants (Fig. 1). The optimized assay parameters are described herein. The common primer pair and probes are detailed in Table 1. This design is intended to enable accurate duplex quantification of both variants in the same well. The design of the assay is illustrated in Fig. 1.

Validation was performed on a Roche LightCycler® 480 II system, using LightCycler® 480 Software (release 1.5.1.62 SP2) for determination of Cp values with manual settings for the noise band and threshold and with color compensation function turned off in order to enhance cross system adaptation. Calculation of parameters was performed using Excel (version 16.16.21, Microsoft, Redmond, CA, USA) and the method described by Pfaffl [13]. The optimal reaction parameters and details of probes and primers are listed in Table 1. The PrimeTime® Gene Expression Master Mix (IDT DNA, Coralville, IA, USA) was used according to manufacturer's recommendation. The total reaction volume was 15 µl. gBlock recombinant DNA for each of XBP-1S and XBP-1U was used to optimize and assess the performance of the assay (IDT DNA) as previously described by Conte *et al.* [14].

Determination of amplification efficacy, detection sensitivity, and interference

Serial dilution of synthetic DNA sequences for both mouse XBP-1S and XBP-1U (gBlocks® IDT DNA) was performed for both the XBP-1S and XBP-1U assays, first alone, then in combination using a grid pattern to analyze the various concentration combinations as detailed in the "Results" section.

MIN6 cell culture

For validation of the assay across varying concentrations of cDNA samples obtained from cells, cDNA was generated from untreated, cultured MIN6 cells (an immortalized insulin-secreting mouse beta-cell line) [15]. Cell culture experiments were conducted as previously described [16]. Briefly, MIN6 cells between passages 29 and 31 were cultured in media containing Dulbecco's modified Eagle's medium (DMEM) (Gibco, Waltham, MA, USA) supplemented with 15% heat-inactivated FBS (Omega Scientific, CA, USA), 100 U/ml penicillin/100 µg/ml streptomycin (Gibco), 2 mmol/l glutamine (Gibco), and 50 µM beta mercaptoethanol (Thermo Fisher).

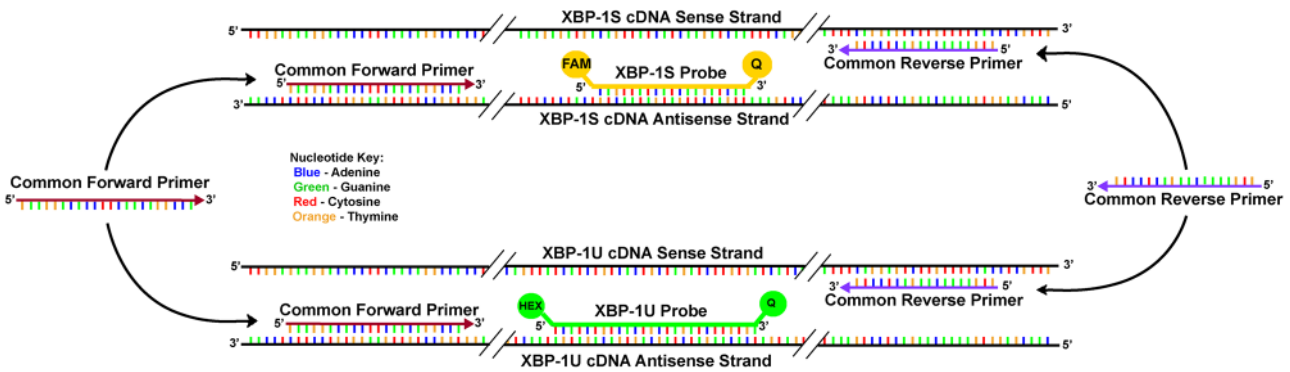

Figure 1: Simplified illustration of the assay design.

Table 1: Technical details of the optimized qPCR assay

Reagents and assay conditions	
XBP-1 forward PCR primer	TGGTTGAGAACCAGGAGTTAAG, final concentration: 500 nM
XBP-1 reverse PCR primer	TCTGGGGAGGTGACAACT, final concentration: 500 nM
XBP-1S-specific hydrolysis fluorescent probe	Probe sequence:/56-FAM/AGTCCGCAG/ZEN/CAGGTGCAGG/3IABkFQ Obtained from IDT DNA (Coralville, IA) Fluorescent dye: HEX Quencher: Iowa Black® FQ and ZEN (IDT DNA) Final concentration: 250 nM
XBP-1U-specific hydrolysis fluorescent probe	5HEX/CAGCACTCA/ZEN/GACTATGTGCACCTCTG/3IABkFQ/ Obtained from IDT DNA (Coralville, IA) Fluorescent dye: FAM Quencher: Iowa Black® FQ and ZEN (IDT DNA) Final concentration: 250 nM
XBP-1S gBlock® synthetic DNA for assay validation (NM_001271730.1)	Gctcgagatagaaagaaagcccggatgagcgagctggagcagcaagtggtggatttggaagaagagaaccacaaactccagctagaaaa tcagcttttacgggagaaaactcacggccttgtggttgagaaccaggagttaagaacacgcttgggaatggacacgctggatcctgac gaggttccagaggtggaggccaaggggagtggagtaaggctggtggccgggtctgctgagtccgcagcaggtgcaggcccagttgtca cctccccagaacatcttcccatggactctgacactgttgcctcttcagattctgagtctgatatccttttgggcattctggacaagttgga ccctgtcatgtttttcaaatgtccttccccagagtctgctag
XBP-1U gBlock® synthetic DNA for assay validation (NM_013842.3, difference from XBP-1S marked by capitalization)	gctcgagatagaaagaaagcccggatgagcgagctggagcagcaagtggtggatttggaagaagagaaccacaaactccagctag aaaatcagcttttacgggagaaaactcacggccttgtggttgagaaccaggagttaagaacacgcttgggaatggacacgctggatcct-gacgaggttccagaggtggaggccaaggggagtggagtaaggctggtggccgggtctgctgagtccgCAGCACTCAGACTAT GTGCACCTCTGcagcaggtgcaggcccagttgtcacctccccagaacatcttcccatggactctgacactgttgcctcttcagattct-gagtctgatatccttttgggcattctggacaagttggaccctgtcatgtttttcaaatgtccttccccagagtctgctag
Cycle temperatures (Times)	Pre-incubation: 95°C (30 s), denaturing: 95°C (10 s), annealing: 61°C (25 s), amplification: 72°C (10 s)
Detection filter wavelengths, noise band, and threshold settings for XBP-1S (FAM)	Readout filter: 465–510 nm, Noise band: 0.5, Threshold for Cp determination: 0.7 (on Roche LightCycler® 480 II system, analysis using LightCycler 480 Software release 1.5.1.62 SP2 for analysis), color compensation function turned off
Detection filter wavelengths, noise band, and threshold settings for XBP-1U (HEX)	Readout filter: 533–580 nm, Noise band: 0.25, Threshold for Cp determination: 0.5(on Roche LightCycler® 480 II system, analysis using LightCycler 480 Software release 1.5.1.62 SP2 for analysis), color compensation function turned off

ER stress mouse model

For validation of our assay in murine hepatic tissue samples, ER stress positive and negative controls from a previous study were remeasured using the new assay. The details of this study were previously reported [17, 18]. In brief, 8-week-old male C57Bl/6J mice were injected with either tunicamycin 0.5 mg/kg or vehicle (20% DMSO/PBS) intraperitoneally and livers were harvested 6 h later. Liver samples were frozen in liquid nitrogen until mRNA extraction. All experiments were approved by the Northwestern University ACUC.

mRNA extraction and cDNA synthesis

mRNA extraction and cDNA synthesis were performed as described previously using the RNeasy easy kit (Qiagen, Hilden, Germany) that was used according to manufacturer's recommendations. DNAse treatment was performed using the DNAse I kit (New England Biolabs, Ipswich, MA, USA) that were used according to manufacturer's recommendations. Reverse transcription was performed using the qScript cDNA synthesis kit (Quantabio, Gaithersburg, MD, USA).

Data analysis

Data analysis was conducted using method described by Pfaffl [13]. The Cp values were averaged between replicate wells prior to calculation as recommended by Schmittgen and Livak [19]. Cp values are used to calculate absolute and relative readout values for XBP-1S and XBP-1U [13].

Results

Optimal assay concentrations and parameters

The sequences and optimal reaction parameters are detailed in Table 1. The optimal final primer concentration for both primers in the reaction mix was 500 nM. The optimal concentration for both hydrolysis probes is 250 nM. The PrimeTime® Gene Expression Master Mix (IDT DNA) was used according to manufacturer's recommendation at a ratio of 1:1 without modifications or addition of any other buffers or salts.

Amplification efficacy of XBP-1S and XBP-1U

The amplification efficacy was assessed using serial dilution (10^3, 10^4, 10^5, 5×10^5, 10^6, 10^7 fmol/l) of each S and U variant sequences using synthesized murine XBP-1S and XBP-1U sequences (NM_001271730.1 and NM_013842.3, IDT DNA, Table 1). This concentration range was chosen based on concentrations established in typical mRNA preparations from cultured MIN6 cells as well as primary murine liver tissue, see below. The amplification efficacy was 1.88 ± 0.017 and 1.96 ± 0.048 for the S and U variant, respectively, when each were amplified alone without the presence of the other (Table 2, amplification efficacy of 2 corresponds to 100% amplification per cycle).

Dynamic detection range and amplification efficacy for XBP-1S in the presence of varying XBP-1U concentration and vice versa

To examine for possible interference between both XBP-1 splice variants within the dynamic range of the assay, the amplification

Table 2: Amplification efficiency scores, quantitative and semi-quantitative detection range, and cross detection for (a) XBP-1U at varying XBP-1S cDNA template concentrations and of (b) XBP-1S at varying XBP-1U cDNA template concentrations

(a) Performance characteristics of the XBP-1U detection probe

XBP-1S cDNA template concentration	Amplification efficiency score for XBP-1U at the XBP-1S template concentration specified in column 1 ±SEM	Range for XBP-1U accurate quantitative detection at the XBP-1S template concentration listed in column 1	XBP-1U semi-quantitative detection range at the XBP-1S template concentration listed in column 1	Cross detection readout of XBP-1S template by the XBP-1U probe at the XBP-1S concentration listed in column 1 in the absence of XBP-1U template
0 fmol/l	1.96 ± 0.048	10^3–10^7 fmol/l	N/A	None
10^3 fmol/l	1.91 ± 0.035	10^3–10^7 fmol/l	N/A	None
10^4 fmol/l	1.91 ± 0.039	10^3–10^7 fmol/l	N/A	None
10^5 fmol/l	1.86 ± 0.036	10^4–10^7 fmol/l	10^3–10^4 fmol/l	None
5×10^5 fmol/l	1.82 ± 0.049	10^5–10^7 fmol/l	10^3–10^5 fmol/l	None
10^6 fmol/l	1.79 ± 0.056	5×10^5–10^6 fmol/l	10^3–5×10^5 fmol/l	None
10^7 fmol/l	Could not be accurately determined	10^7 fmol/l	10^4–10^7 fmol/l	Cross detection value of 10^3

(b) Performance characteristics of the XBP-1S detection probe

XBP-1U cDNA template concentration	Amplification efficiency score for XBP-1S at tde XBP-1U template concentration specified in column 1 ±SEM	Range for XBP-1S accurate quantitative detection at tde XBP-1U template concentration listed in column 1	XBP-1S semi-quantitative detection range at tde XBP-1U template concentration listed in column 1	Cross detection readout of XBP-1U template by tde XBP-1S probe at tde XBP-1S concentration listed in column 1 in tde absence of XBP-1S template
0 fmol/l	1.88 ± 0.017	10^3–10^7 fmol/l	N/A	None
10^3 fmol/l	1.87 ± 0.015	10^3–10^7 fmol/l	N/A	None
10^4 fmol/l	1.88 ± 0.027	10^3–10^7 fmol/l	N/A	None
10^5 fmol/l	1.84 ± 0.032	10^4–10^7 fmol/l	10^3–10^4 fmol/l	None
5×10^5 fmol/l	1.81 ± 0.011	10^5–10^7 fmol/l	10^3–10^5 fmol/l	None
10^6 fmol/l	1.84 ± 0.03	10^5–10^7 fmol/l	10^3–10^5 fmol/l	None
10^7 fmol/l	1.73 ± 0.03	5×10^5–10^7 fmol/l	10^3–5×10^5 fmol/l	None

An amplification efficiency score of 2 translates to an amplification efficiency of 100% per cycle. The range of accurate quantitative detection is defined as the concentration range of the template where the ratio of detected versus actual concentration is between 0.5 and 2. The semi-quantitative (non-linear) detection range is defined as the template concentration range where the ratio of detected versus actual concentration is outside of the 0.5–2 range but the rank order of input concentrations is detected accurately, resulting in the output producing an accurate rank order of concentration readouts but not a fully linear readout. The cross detection depicts the inappropriate readout level of a XBP-1U signal in the absence of XBP-1U template at the XBP-1S template concentration listed in the (a) first column and (b) vice versa.

efficacy of XBP-1U in the presence of increasing XBP-1S concentrations and the amplification efficacy of XBP-1S in the presence of increasing XBP-1U concentrations were determined.

The dynamic range for the accurate detection for each XBP-1S and XBP-1U across the concentration range of 10^3 and 10^7 fmol/l was assessed (Table 2). The detection dynamic range was sufficient for the accurate detection of each variant across XBP-1S to XBP-1U and XBP-1U to XBP-1S gradients that would be expected in biological specimens. The presence of one splice variant inhibited the detection of the counter variant only to a marginal degree. This is not expected to skew readout results under realistic biological conditions in a meaningful way. Only when very high concentration gradients that are beyond the range found in biological specimens are reached, was the limit of accurate quantitative detection reached (Table 2). The directionality of detected change outside this dynamic range continued to be accurate outside this range, thereby providing readout values that are semi-quantitatively accurate (i.e. they are able to accurately detect the directionality of concentration change, though not in a quantitatively accurate fashion). The dynamic range and range of semi-quantitative detection across gradient experiments are summarized in Table 2. Figure 2 depicts the relationship of input concentration of each of XBP-1U and XBP-1S and their detected concentrations at various concentrations of the counterpart in the same well. The amplification efficacies are affected only marginally as long as the concentration of a splice variant remains within the dynamic range of the assay (Table 2 and Fig. 2).

Assessment of cross detection

No cross detection of XBP-1U by the XBP-1S probe was detected (Table 2). XBP-1S was detected by the XBP-1U probe only when the highest XBP-1S concentration of 10^7 fmol/l was reached. At this concentration, a XBP-1U signal of 10^3 fmol/l was detected. It is unlikely that this will have a significant impact under most biological conditions.

Assay validation using normal biological samples in serial dilution

Next, we investigated the assay performance using real life biological samples. We generated cDNA from untreated MIN6 cell mRNA. We measured the concentration for XBP-1S and XBP-1U by performing serial dilutions of these samples (1, 0.5, 0.25, 0.125, and 0.0625). This showed values for XBP-1S and XBP-1U and their ratios that are consistent with their dilution. The

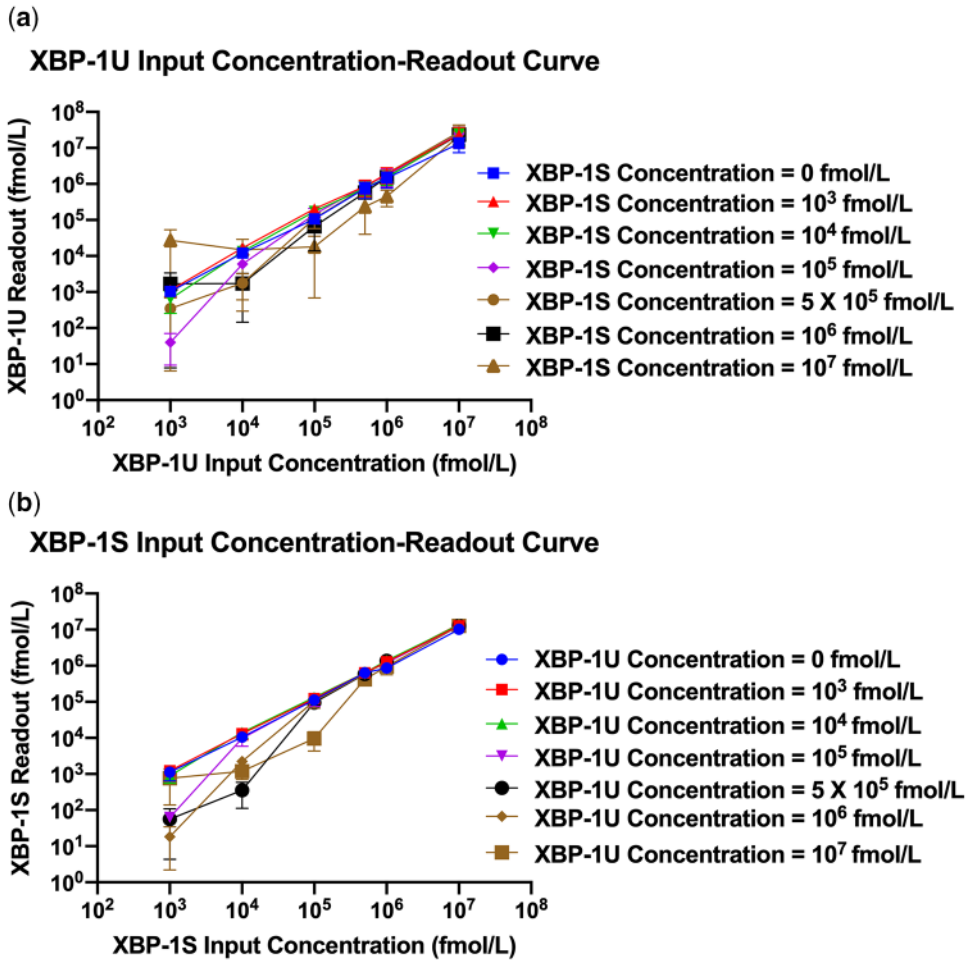

Figure 2: Correlation between input concentration and assay quantification of XBP-1U DNA in the presence of varying concentrations of (a) XBP-1S DNA and (b) vice versa, $n = 3$, data points and error bars represent mean ± SEM.

readout values were values relative to undiluted 1.000 XBP-1U. For XBP-1S, the readout values were (normalized to undiluted XBP-1U): 0.161 ± 0.083, 0.093 ± 0.0166, 0.047 ± 0.017, 0.026 ± 0.008, and 0.01 ± 0.002. For XBP-1U, the readout values were: 1.0 ± 0, 0.488 ± 0.011, 0.194 ± 0.001, 0.125 ± 0.02, and 0.38 ± 0.00025 (Fig. 3).

Assay validation using cDNA from mouse liver following exposure to tunicamycin

To validate our assay in tissue samples in an ER stress model, ER stress positive and negative controls from a previous *in vivo* study in mice [17, 18] were remeasured using the newly established assay. Eight-week-old male C57Bl/6 mice were injected with either tunicamycin 0.5 mg/kg or vehicle intraperitoneally and harvested 6 h later. Results are summarized in Fig. 4. Consistent with prior observations, absolute values for XBP-1S increased and XBP-1U values decreased, resulting in a marked increase in XBP-1S-to-U ratio in mice exposed to tunicamycin. This is consistent with expected previously reported observations [17, 18].

Discussion

Herein, we report the establishment of a single-common primer pair, dual probe, single well, duplex qPCR assay for the measurement of the relative levels of XBP-1S and XBP-1U. This assay, in addition to being valuable for measuring XBP-1 splice variants, will serve as a proof of concept for this design for use in qPCR. It is similar in conceptual design to a single primer pair, dual probe setup previously established by Sun *et al.* [11] for use in ddPCR for the quantification of hTERT splice variants [12]. It will pave the way for the development of simplified assays for measuring splice variants of other mRNA transcripts using qPCR. An important feature of the assay is the use of a single primer pair for the amplification of both the S and U variants (Fig. 1). The advantage of this setup is that the amplification efficacy is similar for both XBP-1S and XBP-1U, as confirmed by our data (Fig. 2). This allows reliable assessment of their ratio across a broad concentration range.

One important concern when designing a probe-based, duplex, single well assay is cross detection. The pair of S and U probes reported here shows no cross-reactivity across a broad concentration range that encompasses physiologically relevant values when analyzing cDNA from cell lysates with the exception of minimal cross detection of XBP-1S by the XBP-1U probe at extremely high concentration difference of $1{:}10^4$ (Table 2). We do not anticipate that this will result in meaningful skewing under concentration ranges within experimental conditions.

There was a small amount of signal cross inhibition when the concentration ratio of XBP-1S and XBP-1U was high. Nevertheless, the detection continued to be accurate in a semi-quantitative fashion, with low skewing. As a result, we do not anticipate this to be an issue given that the concentration ratio

is much lower under physiological conditions. When assessing serial dilutions of cell lysates, we find that the ratio is sufficiently stable across various dilutions as long as the cDNA concentration is within a concentration range generally used for qPCR. More importantly, the presence of higher concentrations of either U or S slightly diminishes the S or U signal, respectively, rather than increasing it. The cause of signal cross suppression is unclear. We speculate that high concentration of one of the two XBP-1 variants results in the release of larger quantities of the quencher molecule from the hydrolysis probe, possibly leading to quenching of the signal from the other, thereby lowering concentrations of the fluorescence probe following its hydrolysis. Using a lower primer concentration in initial experiments did not mitigate this.

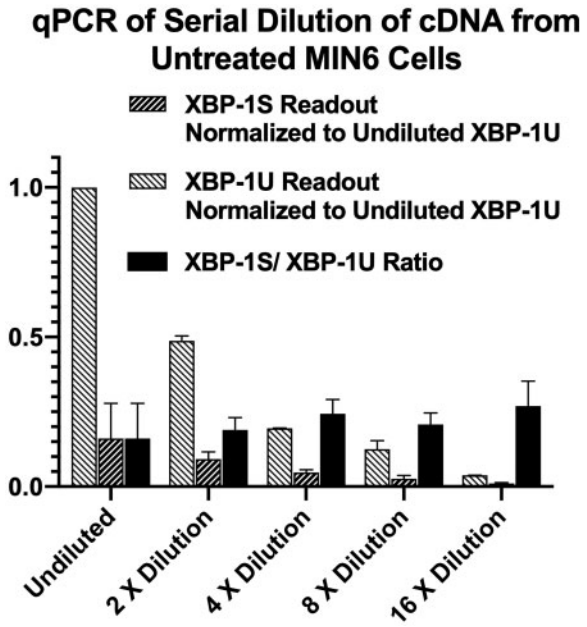

Figure 3: Assay readout for various dilutions of cDNA from untreated MIN6 cells. XBP-1U and XBP-1S concentrations were normalized to undiluted XBP-1U to correct for varying concentrations across experiments [data presented as means±standard deviation (SD)] $n = 2$.

Important differences between qPCR and ddPCR should be considered when choosing between the two options. ddPCR is more sensitive, provides an absolute quantitative readout, and is less susceptible to interference. On the other hand, qPCR is more affordable and widely accessible as well as providing a wider dynamic output range [20].

Measuring the two splicing variants of XBP-1, XBP-1S, and XBP-1U is relevant to many research projects that examine the physiology and pathophysiology of protein misfolding and ER stress [5, 6, 21, 22]. Production of protein-based cell products results in a small percentage of misfolded or misprocessed precursor peptides. Under normal conditions, the cellular machinery has efficient, finely regulated pathways for disposing of these misfolded proteins. However, under certain circumstances, increased quantities of misfolded proteins may lead to these pathways becoming overloaded, resulting in ER stress. ER stress is postulated to contribute to the pathogenesis of several disease states [6, 17, 18, 21, 22]. Detecting factors that cause or exacerbate ER stress is therefore of importance to many investigators. The mRNA of the XBP-1 gene is alternatively spliced during ER stress and serves as a sensitive and reliable marker of early ER stress. The classical method for quantifying XBP-1S-to-XBP-1U ratios, namely Western blotting or semi-quantitative PCR followed by gel electrophoresis is challenging and time-consuming. Recently, qPCR using intercalating dyes such as SYBR green have gained popularity. Our newly validated duplex,

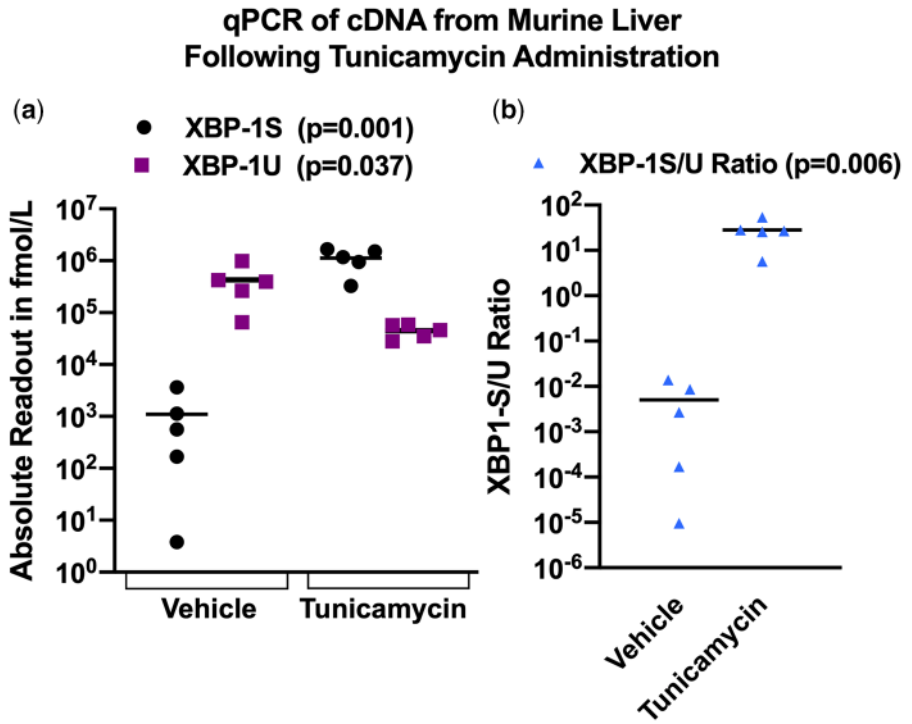

Figure 4: Readout of (a) XBP-1U and XBP-1S as well as (b) the calculated XBP-1S/U ratio in murine liver samples from a previously published study of tunicamycin-induced ER stress, remeasured using the assay described herein ($n = 5$). Horizontal lines represent the means.

single primer pair, dual probe-based qPCR assay improves on this approach. Specifically, it enables single well measurement of both variants simultaneously in the same well by using a probe with a distinct wavelength for the detection of each variant. The performance parameters of the assay as reported here show that the assay provides accurate quantification of mouse XBP-1S and XBP-1U within the concentration range expected under normal physiological conditions as well as under conditions of ER stress as demonstrated in cDNA generated from murine liver under normal and ER stress conditions (Fig. 4). While the current assay design was established in murine homolog of XBP-1, we anticipate that adapting this assay for human, rat, and other species will likely be straightforward. Specifically, the inter-species sequence homology in the region of primers and probes differs only by a few base pairs. Therefore, we anticipate that using parameters established in the assay reported herein as a starting point will simplify such an effort.

In summary, here we present a proof of concept probe-based, qPCR assay for measuring the ratio of murine XBP-1S and XBP-1U that can be performed in a single well format, thereby enhancing reproducibility and accuracy.

Data Availability

The data underlying this article are available in the article and in its online Supplementary Material.

Supplementary data

Supplementary data is available at *Biology Methods and Protocols* online.

Author contributions

J.W.: conceptualization, data curation, investigation, methodology, project administration, resources, validation, and review and editing. W.P.W.: conceptualization, investigation, methodology, project administration, resources, supervision, and review and editing. E.O.L.: data curation, investigation, methodology, validation, and review and editing. S.O.: investigation, methodology, validation, and writing—review and editing. C.T.A.: data curation, formal analysis, visualization, and writing—review and editing. A.S.H.: data curation, investigation, resources, supervision, validation, and review and editing. M.E.M.: conceptualization, formal analysis, funding acquisition, investigation, methodology, resources, supervision, visualization, writing original draft, and writing—review and editing.

Acknowledgements

Funding was provided by the US National Institute of Health/The National Institute for Environmental Health Sciences (NIH/NIEHS) for M.E.M., J.W., and W.P.W. (Grant No. 5R01ES027011).

Conflict of interest statement. None declared.

References

1. West S, Kumar S, Batra SK *et al.* Uncovering and characterizing splice variants associated with survival in lung cancer patients. *PLoS Comput Biol* 2019;**15**:e1007469.
2. Dudley RJ, Smalldon KW. The objective comparison of the particle size distributions in soils with particular reference to the sand fraction. *Med Sci Law* 1978;**18**:278–82.
3. Stevens M, Oltean S. Alternative splicing in CKD. *JASN* 2016; **27**:1596–603.
4. Deschenes M, Chabot B. The emerging role of alternative splicing in senescence and aging. *Aging Cell* 2017;**16**:918–33.
5. Lee K, Tirasophon W, Shen X *et al.* IRE1-mediated unconventional mRNA splicing and S2P-mediated ATF6 cleavage merge to regulate XBP1 in signaling the unfolded protein response. *Genes Dev* 2002;**16**:452–66.
6. Olivares S, Henkel AS. Induction of fibroblast growth factor 21 does not require activation of the hepatic X-box binding protein 1 in mice. *Mol Metab* 2017;**6**:1616–24.
7. Yoon SB, Park YH, Choi SA, *et al.* Real-time PCR quantification of spliced X-box binding protein 1 (XBP1) using a universal primer method. *PLoS ONE* 2019;**14**:e0219978.
8. Samali A, Fitzgerald U, Deegan S *et al.* Methods for monitoring endoplasmic reticulum stress and the unfolded protein response. *Int J Cell Biol* 2010;**2010**:1–11.
9. Vandenbroucke II, Vandesompele J, Paepe AD *et al.* Quantification of splice variants using real-time PCR. *Nucleic Acids Res* 2001;**29**:E68–E68.
10. Camacho Londono J, Philipp SE. A reliable method for quantification of splice variants using RT-qPCR. *BMC Mol Biol* 2016;**17**.
11. Sun B, Tao L, Zheng YL. Simultaneous quantification of alternatively spliced transcripts in a single droplet digital PCR reaction. *Biotechniques* 2014;**56**:319–25.
12. Sun B, Zheng YL. Simultaneous quantification of multiple alternatively spliced mRNA transcripts using droplet digital PCR. *Methods Mol Biol* 2018;**1768**:387–400.
13. Pfaffl MW. A new mathematical model for relative quantification in real-time RT-PCR. *Nucleic Acids Res* 2001;**29**:e45.
14. Conte J, Potoczniak MJ, Tobe SS. Using synthetic oligonucleotides as standards in probe-based qPCR. *Biotechniques* 2018;**64**: 177–9.
15. Miyazaki J, Araki K, Yamato E *et al.* Establishment of a pancreatic beta cell line that retains glucose-inducible insulin secretion: special reference to expression of glucose transporter isoforms. *Endocrinology* 1990;**127**:126–32.
16. El Muayed M, Billings LK, Raja MR *et al.* Acute cytokine-mediated downregulation of the zinc transporter ZnT8 alters pancreatic beta-cell function. *J Endocrinol* 2010;**206**:159–69.
17. Henkel AS, LeCuyer B, Olivares S *et al.* Endoplasmic reticulum stress regulates hepatic bile acid metabolism in mice. *Cell Mol Gastroenterol Hepatol* 2017;**3**:261–71.
18. Olivares S, Green RM, Henkel AS. Endoplasmic reticulum stress activates the hepatic activator protein 1 complex via mitogen activated protein kinase-dependent signaling pathways. *PLoS ONE* 2014;**9**:e103828.
19. Schmittgen TD, Livak KJ. Analyzing real-time PCR data by the comparative C(T) method. *Nat Protoc* 2008;**3**:1101–8.
20. Taylor SC, Laperriere G, Germain H. Droplet digital PCR versus qPCR for gene expression analysis with low abundant targets: from variable nonsense to publication quality data. *Sci Rep* 2017;**7**:2409.
21. Hoyer-Hansen M, Jaattela M. Connecting endoplasmic reticulum stress to autophagy by unfolded protein response and calcium. *Cell Death Differ* 2007;**14**:1576–82.
22. Olivares S, Henkel AS. Hepatic Xbp1 gene deletion promotes endoplasmic reticulum stress-induced liver injury and apoptosis. *J Biol Chem* 2015;**290**:30142–51.